UNCLASSIFIED

(2)

AD-A202 954

REPORT DOCUMENTATION PAGE

1b. RESTRICTIVE MARKINGS

AFOSR, FILE COPY

3. DISTRIBUTION/AVAILABILITY OF REPORT
Approved for public release:
Distribution unlimited

2b. DECLASSIFICATION/DOWNGRADING SCHEDULE

4. PERFORMING ORGANIZATION REPORT NUMBER(S)

5. MONITORING ORGANIZATION REPORT NUMBER(S)
AFOSR-TR- 88-1255

6a. NAME OF PERFORMING ORGANIZATION
EMORY UNIVERISITY

6b. OFFICE SYMBOL (If applicable)

7a. NAME OF MONITORING ORGANIZATION
AFOSR/NC

6c. ADDRESS (City, State and ZIP Code)
1515 Pierce Drive
Atlanta, GA 30322

7b. ADDRESS (City, State and ZIP Code)
Building 410
Bolling AFB, DC 20332-6448

8a. NAME OF FUNDING/SPONSORING ORGANIZATION
AFOSR

8b. OFFICE SYMBOL (If applicable)
NC

9. PROCUREMENT INSTRUMENT IDENTIFICATION NUMBER
AFOSR-87-0197

8c. ADDRESS (City, State and ZIP Code)
Building 410
Bolling AFB, DC 20332-6448

10. SOURCE OF FUNDING NOS.

PROGRAM ELEMENT NO.	PROJECT NO.	TASK NO.	WORK UNIT NO.
61102F	2303	B1	

11. TITLE (Include Security Classification)
Spectroscopy and Energy Transfer Kinetics of the Interhalogens

12. PERSONAL AUTHOR(S)
Michael C. Heaven

13a. TYPE OF REPORT	13b. TIME COVERED	14. DATE OF REPORT (Yr., Mo., Day)	15. PAGE COUNT
Final	FROM 6/1/87 TO 7/1/88	10/20/88	43

16. SUPPLEMENTARY NOTATION

17. COSATI CODES		
FIELD	GROUP	SUB. GR.

18. SUBJECT TERMS (Continue on reverse if necessary and identify by block number)
Chemical lasers, Halogens,
Metastable States, Interhalogens
Energy Transfer, Singlet Oxygen, IOCl

19. ABSTRACT (Continue on reverse if necessary and identify by block number)
(see reverse)

20. DISTRIBUTION/AVAILABILITY OF ABSTRACT
UNCLASSIFIED/UNLIMITED ☒ SAME AS RPT ☒ DTIC USERS ☐

21. ABSTRACT SECURITY CLASSIFICATION
Unclassified

22a. NAME OF RESPONSIBLE INDIVIDUAL	22b TELEPHONE NUMBER (Include Area Code)	22c OFFICE SYMBOL
F. J. Wodarczyk	202/767-4963	NC

DD FORM 1473, 83 APR EDITION OF 1 JAN 73 IS OBSOLETE.

UNCLASSIFIED
SECURITY CLASSIFICATION OF THIS PAGE

19. ABSTRACT

The spectroscopy, fluorescence decay lifetimes, and energy transfer dynamics of electronically excited I_2 and IBr have been investigated in solid rare gas matrices (Rg = Ar, Kr, and Xe).

Visible laser excitation (460-800 nm) of dilute Rg/I_2 (1000:1) matrices resulted in emission from the I_2 $A^3\Pi(1_u)$ state. Re-analysis of the $A \rightarrow X$ spectra provided revised molecular constants for matrix isolated I_2. A state lifetimes of 70 ± 20, 80 ± 20, and 110 ± 30 μs were observed in Ar, Kr, and Xe hosts respectively. The A state excitation spectrum closely followed the I_2 continuum absorption spectrum, indicating that transfer from the $B^3\Pi(0_u^+)$ and $^1\Pi(1_u)$ states was effective in populating $I_2(A)$. At dilution ratios of 600:1 or lower the I $^2P_{1/2}$ - $^2P_{3/2}$ transition was observed in conjunction with the A-X bands. Excitation studies showed that isolated I atoms, trapped during the deposition process, were excited by electronic energy transfer from nearby I_2^* molecules. A vibronic progression, similar to that of the A-X bands, but shifted to longer wavelengths, was noted in concentrated Rg/I_2 matrices (300:1). This system, which was emitted with a lifetime of about 10 ms, most probably originated from iodine dimers or I_3.

Excimer laser excitation (193 nm) of dilute Ar/I_2 matrices produced a single, intense vibronic feature at 380 nm, the I_2 A-X bands, and the I $^2P_{1/2}$ - $^2P_{3/2}$ line. The uv emission exhibited a lifetime of about 5 ns, and was tentatively identified as the $D'^3\Pi(2g)$ - $A'^3\Pi(2u)$ transition. This assignment implies a gas phase to matrix red-shift of about 3100 cm^{-1}. With 193 nm excitation the atomic line was most probably produced by direct photodissociation. Intermolecular energy transfer processes were not observed in dilute matrices.

Laser excitation of Ar/IBr matrices at wavelengths within the 420-610 nm range, resulted in emission from the IBr B-X and A-X systems. The former was completely diffuse, while the A-X bands formed a single vibronic progression from 980-1500 nm. Analysis of this progression revealed a matrix red-shift of $T_e(A)$ by 310 cm^{-1}, and minimal perturbation of the ground state vibrational constants (ω_e = 268, $\omega_e x_e$ = 1.04 cm^{-1}). Energy from IBr(A) to I $^2P_{1/2}$ was observed in concentrated matrices.

COMPLETED PROJECT SUMMARY

TITLE: The Spectroscopy and Energy Transfer Kinetics of the Interhalogens

PRINCIPAL INVESTIGATOR: Dr. Michael C. Heaven
Department of Chemistry
Emory University
Atlanta, Georgia 30322

COSTS AND FY SOURCE: $64,678, FY87

SENIOR RESEARCH PERSONNEL: Dr. Wafaa M. Fawzy

JUNIOR RESEARCH PERSONNEL: Mr. Michel Macler

PUBLICATIONS:

"Electronic Spectroscopy and Energy Transfer Pathways of Matrix Isolated I_2", W. M. Fawzy, M. Macler, J. P. Nicolai, and M. C. Heaven, J. Chem. Phys., submitted.

"Laser Excitation and Resolved Fluorescence Spectra for Matrix Isolated IBr", M. Macler and M. C. Heaven, in preparation.

"Ultraviolet Emission Spectra from Matrix Isolated I_2", M. Macler and M. C. Heaven, in preparation.

ABSTRACT OF OBJECTIVES AND ACCOMPLISHMENTS:

The objective of this program has been the determination of spectroscopic and radiative lifetime data for the low energy, metastable states of the halogens and interhalogens. This information was obtained by recording wavelength and time resolved laser excitation spectra for molecules isolated in rare gas matrices.

The spectroscopy, fluorescence decay lifetimes, and energy transfer dynamics of electronically excited I_2 and IBr have been investigated in solid rare gas matrices (Rg = Ar, Kr, and Xe). Visible laser excitation (460-800 nm) of dilute Rg/I_2 (1000:1) matrices resulted in emission from the I_2 $A^3\Pi(1_u)$ state. Re-analysis of the A→X spectra provided revised molecular constants for matrix isolated I_2. A state lifetimes of 70 ± 20, 80 ± 20, and 110 ± 30 μs were observed in Ar, Kr, and Xe hosts respectively. The A state excitation spectrum closely followed the I_2 continuum absorption spectrum, indicating that transfer from the $B^3\Pi(0_u^+)$ and $^1\Pi(1_u)$ states was effective in populating $I_2(A)$. At dilution ratios of 600:1 or lower the I $^2P_{1/2}$ - $^2P_{3/2}$ transition was observed in conjunction with

the A-X bands. Excitation studies showed that isolated I atoms, trapped during the deposition process, were excited by electronic energy transfer from nearby I_2 molecules. A vibronic progression, similar to that of the A-X bands but shifted to longer wavelengths, was noted in concentrated Rg/I_2 matrices (300:1). This system, which was emitted with a lifetime of about 10 ms, most probably originated from iodine dimers or I_3.

Excimer laser excitation (193 nm) of dilute Ar/I_2 matrices produced a single, intense vibronic feature at 380 nm, the I_2 A-X bands, and the $I\ ^2P_{1/2} - ^2P_{3/2}$ line. The uv emission exhibited a lifetime of about 5 ns, and was tentatively identified as the $D'^3\Pi(2g) - A'^3\Pi(2u)$ transition. This assignment implies a gas phase to matrix red-shift of about 3100 cm^{-1}. With 193 nm excitation the atomic line was produced by direct photodissociation. (Intermolecular energy transfer processes were not observed in dilute matrices.)

Laser excitation of Ar/IBr matrices at wavelengths within the 420-610 nm range, resulted in emission from the IBr B-X and A-X systems. The former was completely diffuse, while the A-X bands formed a single vibronic progression from 980-1500 nm. Analysis of this progression revealed a matrix red-shift of Te(A) by 310 cm^{-1}, and minimal perturbation of the ground state vibrational constants ($\omega_e = 268$, $\omega_e x_e = 1.04$ cm^{-1}). Energy transfer from IBr(A) to $I\ ^2P_{1/2}$ was observed in concentrated matrices.

I. Introduction

The diatomic halogens and interhalogens can be used as active media in short wavelength laser systems. They can be stimulated to lase by optical, electron impact, or chemical means of excitation. The excitation mechanisms involve many low-lying electronic states (i.e. $B^3\Pi(0^+)$, $A^3\Pi(1)$, $A'^3\Pi(2)$) and, in some instances, the high energy ion-pair states. Spectroscopic and kinetic characterizations of many of the states are required to gain a further understanding of these demonstrated laser systems, and an assessment of the potential of new systems.

In recent years we have been using laser excitation of matrix isolated halogens and interhalogens as a means for investigating the metastable states arising from the 2431 electronic configuration. The matrix environment offers a number of unique properties which are particularly useful for the study of weak or forbidden transitions. Rapid transfer between overlapping electronic states is induced by the matrix, so that initial excitation of an allowed transition can result in population of states which are inaccessible due to selection rules or Franck-Condon restrictions. Vibrational relaxation is very fast in the matrix, and the emission spectra usually originate from v'=0. Thus simple progressions are obtained for each electronic state populated. Excitation to repulsive states can also be used to populated bound states. Complete dissociation is prevented by the matrix cage, and the atoms are constrained to recombine into a variety of electronic states. These properties have been exploited in studies of the **B**, **A**, and/or **A'** states of I_2,[1-4] Br_2,[5-11] Cl_2,[5,12] ICl,[13,14] and IF.[15,16]

During the past year we have made further studies of the electronic spectra of matrix isolated I_2. The objectives of this work have been characterization of the **A-X** and **D'-A'** emission systems, and studies of the condensed-phase energy transfer from electronically excited I_2 to $I^2P_{1/2}$ and $O^2(a^1\Delta)$. The transfer

processes were examined as they are of relevance to the chemically pumped oxygen iodine laser.

Electronic spectra for matrix isolated IBr have also been investigated. Fluorescence from the **B** and **A** states, and energy transfer from IBr(**A**) to $I^2P_{1/2}$ was observed. Significant similarities in the behavior of IBr(**B**) and I_2(**B**) in rare-gas matrices were noted. They indicate that predissociation of the **B**, v'=0 level plays an important role in the condensed phase relaxation dynamics.

II. Experimental

The matrix isolation system used for this work has been described previously.[16] Mixtures of I_2 diluted in a rare gas host (Rg = Ar, Kr, or Xe) were deposited on a gold plated copper disk held at temperatures between 10 and 20 K. Dilution ratios (Rg:I_2) in the range of 300:1 to 2000:1 were investigated. Preparation of suitable IBr samples was slightly more involved. IBr cannot be obtained in a pure form as it exists in equilibrium with I_2 and Br_2. From a spectroscopic viewpoint the presence of I_2 is troublesome, as it has intense spectra throughout the region where the IBr bands are expected. On the other hand, the presence of excess Br_2 can be tolerated, as its band systems are considerably weaker than those of IBr. Therefore, excess Br_2 was added to the IBr samples in order to minimize the concentration of free I_2. Typically, good results were achieved with samples consisting of 2000:1:10, Ar:IBr:Br_2.

For the majority of the experiments reported here, the matrices were excited by pulses from a Nd/YAG laser (Quanta-Ray DCR1), or a YAG pumped dye laser (Quanta-Ray PDL1). An ArF excimer laser (Lumonics TE-861-4) was used to excite the ion-pair states of I_2. Fluorescence from the matrices was imaged onto the slits of a 0.25 m monochromator (Bausch and Lomb). Long-pass colored glass filters were used to block laser scatter light. Light emerging from the

monochromator was detected by either a liquid nitrogen cooled germanium detector (ADC model 403, range 700-1600 nm), or a GaAs photomultiplier (RCA 4832, range 350-950 nm). Signals from the detectors were processed by a boxcar integrator (SRS250) for the recording of excitation spectra, resolved fluorescence spectra, and fluorescence decay curves with lifetimes in excess of 5 ms. Faster decays were captured in real time by a transient recorder (Le Croy TR8837F) and signal averaged by a microcomputer (Zenith ZW-158).

Excitation spectra and fluorescence decay curves were obtained by monitoring the intensities of isolated vibronic features (fixed wavelength detection). Excitation spectra were corrected for the wavelength dependence of the dye laser intensity by monitoring the fluorescence intensity vs. laser power ratio. A calometric power meter (Scientech model 36-0201) was used for this purpose. Wavelength resolved fluorescence spectra were recorded by scanning the monochromator while the excitation wavelength was held constant.

III. Visible laser excitation of matrix isolated I_2

III. a. Results

(i) Dilute Matrices

Resolved fluorescence spectra for dilute (2000:1) Rg:I_2 matrices are shown in Fig. 1. Complete vibronic resolution of the spectra could not be achieved, as the features exhibited linewidths of 100 cm^{-1} (FWHM) in all three matrix hosts. In each host the vibronic structure was particularly simple, consisting of a single progression with the intensity distribution characteristic of emission originating from v'=0 of the excited state. Average vibronic band centers, determined from data taken from several different matrices, are listed in Table 1. These bands were also reported by Beeken et al.,[4] who provided convincing arguments for assigning them to the I_2 A-X system. Figure 2 shows the A state excitation

spectrum. This was not studied systematically for wavelengths greater than 600 nm, but single photon **A** state excitation was observed between 600 and 725 nm.

Attempts to measure the **A** state fluorescence decay rate were complicated by the slow response of the Ge detector and its pre-amplifier. The instrumental response was characterized by examining signals produced by scattered 1064 nm pulses (10 ns duration) from the laser. A bi-exponential curve was obtained which reached a maximum after 120 μs, and followed the form

$$I = k(e^{-t/\tau_1} - e^{-t/\tau_2}),$$

where k is a constant, τ_1 is the fall time, and τ_2 is the rise time. Non-linear least squares fitting of the response curve gave τ_1 = 1.6 ms and τ_2 = 30 μs.

The effects of convoluting the **A** state fluorescence decay with the instrumental response were easily recognized in the time resolved signals from the **A-X** bands. Compared to the curves for scattered laser light, these signals had slower rise times, and reached their maxima after longer delays. For example, the maximum of the 1391 nm (0-17) signal from I_2(**A**) in Ar occurred after 280 μs. Fluorescence decay lifetimes were extracted from the measured curves by fitting to the appropriate tri-exponential equation, with τ_1 and τ_2 fixed at their pre-determined values. Lifetimes of 70 ± 20, 80 ± 20, and 110 ± 30μs were observed in Ar, Kr, and Xe matrices respectively.

(ii) Intermediate Concentration Matrices

Spectra recorded using short boxcar gate delay times (~0.5 ms) showed an interesting gradual change as the concentration was increased from 700:1 to 400:1. The vibrational intervals appeared to widen with increasing concentration, causing the bands at longer wavelength to be successively more red-shifted.

Evolution from the **A-X** bands to the more widely spaced spectrum was complete at a dilution of 400:1. Increasing the concentration from 400:1 to 300:1 produced no further changes in the spectrum. Figure 3 shows examples of the spectra from 300:1, Rg:I_2 matrices. The band centers determined from these spectra are listed in Table 2. The lifetime of the emission also appeared to be strongly dependent on concentration. Lifetimes of 13, 10, and 9 ms were observed in 300:1 Ar, Kr, and Xe matrices, respectively.

Spectra recorded with long gate delay times (>5 ms) exhibited a different concentration dependence. While the intensities of these spectra were approximately quadratically dependent on concentration, the bands always occurred at the positions given in Table 2. It was also found that the fluorescence decay rate, at times greater than 5 ms, was independent of concentration (within the range that allowed observation of the long-lived emission). Hence, the apparent concentration dependence of the 0.5 ms gate delay spectra was seen to be a consequence of the superposition of the two band systems. Excitation spectra for the long-lived emitter were closely similar to those for I_2(**A**).

At dilution ratios below 700:1 the atomic I $^2P_{1/2} \rightarrow {}^2P_{3/2}$ transition was observed. Fig 4 shows a representative spectrum from a 600:1, Ar:I_2 matrix. This trace was recorded with a gate delay of 2 ms, in order to enhance the appearance of the long-lived atomic feature. The positions for the atomic line, measured in 600:1, Ar, Kr, and Xe matrices, are given in Table 3. Prolonged exposure (>3 hrs) of the samples to intense (5 mJ per pulse, 20 Hz) 532 nm radiation did not affect the ratio of atomic to molecular emission.

Fluorescence decay curves were recorded with the monochromator tuned to the center of the atomic line. As the early part of the decay contained components of both molecular and atomic fluorescence, the I $^2P_{1/2}$ lifetime was determined from the decay characteristics at times greater than 5 ms. Lifetimes

of 5 ± 1 ms were seen in 600:1 Ar and Xe matrices. In Kr the decay was appreciably faster, and appeared to be comparable to the detector fall time. Thus only an upper limit of 2 ms could be determined.

Excitation spectra for the atomic line were obtained by monitoring the tail (t>5 ms) of the fluorescence. The results were again similar to the Fig. 2. Power dependence measurements, made throughout the 550-725 nm range, indicated that the atomic emission was produced by single photon absorption.

(iii) $Rg/O_2/I_2$ Matrices

Matrices of $Rg/O_2/I_2$ mixtures were examined in a limited series of experiments. The exact amount of O_2 added to the mixture was not carefully controlled, but approximate ratios of $Rg:O_2:I_2$ of 500-250:50-10:1 were used. Excitation of these samples at wavelengths around 560 nm produced the I_2(A-X), $I(^2P_{1/2} - {}^2P_{3/2})$, and O_2(a-X) emission systems. An example of the fluorescence spectrum from a $Xe/O_2/I_2$ matrix is shown in Fig 5. In Ar, Kr, and Xe the O_2 (a-X), 0-0 band appeared essentially unshifted from its gas-phase position (7882 cm^{-1}). High concentrations of O_2 caused a splitting of the I $(^2P_{1/2} - {}^2P_{3/2})$ line into two components. The first was observed at the position characteristic of pure Rg/I_2 matrices, while the second was red-shifted by a further 140 cm^{-1}. Excitation spectra for O_2(a) were the same as Fig. 2.

The lifetime of O_2(a) was very sensitive to the concentration of I_2. For different samples, lifetimes ranging from about 5s (low I_2 concentration) to 20 ms (high I_2 concentration) were observed. A lengthening of the I^* lifetime in the presence of O_2(a) was also noted.

III. b. Discussion

(i) I_2 (A→X) Emission

Our I_2 A→X spectra were in good agreement with the results of Beeken et al.[4] However, we propose alternative vibrational numberings and revised molecular constants based on the following considerations.

As the A-X bands originated from v'=0, the ground state vibrational constants and numberings were obtained by fitting the data from Table 1 to the equation

$$\upsilon = T_{oo} - \omega''_e v'' + \omega''_e x''_e v''(v'' + 1) \qquad \text{eq. (1)}$$

In the absence of data for more than one isotopic species this procedure defines $\omega_e''x''_e$, but the numbering, T_{oo}, and ω''_e are not uniquely determined. Fortunately, Andrews and co-workers have determined the ω''_e values for I_2 in Ar(213.7 cm^{-1}),[1,2] Kr(211 cm^{-1}),[1] and Xe(211 cm^{-1})[1] by Raman spectroscopy. When the fitting procedures were constrained to reproduce these vibrational frequencies, the numberings were determined to within ±2 units. Further refinements were obtained by comparing the fitted values for T_o with the gas-phase constant. Previous studies of halogens and interhalogens isolated in Ar matrices have shown that the T_{oo} values are decreased by 200-250 cm^{-1} from their gas phase values.[16,17] When this additional restriction was applied in fitting the I_2/Ar data, the numbering given in Table 1 was uniquely determined.

The gas-to-matrix shifts of T_{oo} induced by trapping halogens in Kr and Xe have not been characterized. On the basis of the behavior of a large number of other diatomic molecules,[17] red-shifts which are approximately proportioned to the polarizability of the host are expected. This trend has been observed for the $^2P_{1/2} \rightarrow {}^2P_{3/2}$ transition of matrix isolated I atoms (see below). Consequently, the A-X fits were subjected to the additional constraint of T_{oo} (Ar) > T_{oo} (Kr) > T_{oo} (Xe). The vibrational numberings derived from this scheme are given in Table 1, and the resulting constants and gas-to-matrix shifts are listed in Table 4. All of

our assignments and T_{oo} values differ from those suggested by Beeken et al.,[4] who constrained their fits to minimize the differences between the gas-phase and matrix T_{oo} values.

The **A** state lifetimes obtained in this study were also at variance with those of Beeken at al.[4]; the present results being shorter by a factor of approximately 3. Beeken et al.[4] recorded decay curves with a fast response detector, so their results were not subject to the uncertainties introduced by deconvolution. However, their lifetimes are surprisingly long. When corrected for the effects of the matrix environment they correspond to a gas-phase lifetime in excess of 420 μs. Experimental values for the gas-phase lifetime are not available, but this parameter can be calculated from the transition moment (R_e). Tellinghuisen's[18] value of R_e^2= 0.0407 D^2 yields a lifetime of 220 μs, and it is unlikely that the true lifetime can be much longer. Among the diatomic halogens the radiative decay rates reflect the magnitudes of spin-orbit coupling within the 2431 $^3\Pi$ states.[19] Thus the I_2 (**A**) lifetime is expected to be substantially shorter than the 350 μs lifetime of Br_2(**A**).[20] Extrapolation of the present matrix results gives gas-phase I_2 (**A**) lifetimes of 120 ± 30 (Ar), 150 ± 35 (Kr), and 240 ± 60 μs (Xe). It is possible that the lifetime is shortened by non-radiative decay in Ar and Kr matrices (cf. Br_2 (**A**) in Ar and Kr[6]), but the measurements are not accurate enough to determine this with any confidence.

(ii) **A** State Excitation Spectrum

Within the range of excitation wavelengths examined there are three channels by which the **A** state may be populated. These are;

direct excitation

$$I_2 (X) + h\upsilon \rightarrow I_2 (A), \qquad (1)$$

dissociation followed by geminite recombination

$$I_2\,(X) + h\upsilon \rightarrow I_2\,(^1\Pi(1_u)) \rightarrow 2I(^2P_{3/2}) \rightarrow I_2\,(A), \qquad (2)$$

and transfer from the B state

$$I_2\,(X) + h\upsilon \rightarrow I_2\,(B) \rightarrow I_2\,(A) \qquad (3)$$

For the third channel there are many possible paths by which population could flow from **B→A**.

In Fig. 2 the **A** state excitation spectrum is compared with the absorption spectrum for I_2 in an Ar matrix,[2] and the room temperature gas phase absorption spectrum.[18] The qualitative agreement between the excitation and absorption spectra indicates that channels 1, 2, and 3 are all effective in populating the **A** state. Tellinghuisen[18] has shown that **B-X** absorption dominates between 480-600 nm, so **B→A** transfer must be the most significant excitation channel in this range. Loss of population from matrix isolated I_2 (**B**) is evident in the low fluorescence quantum yield for **B** state emission, the diffuse nature of the **B-X** fluorescence spectrum, and the short-lifetime of the **B** state (~40 ns in an Ar matrix; dramatically reduced from the gas phase value of ~1 μs).[4] This non-radadative decay is consistent with gas phase quenching data for I_2 (**B**), and the collision induced predissociation (CIP) model used to account for deactivation.[21,22] CIP quenching rate constants are dependent on the vibrational state through vibrational wavefunction overlap integrals.[21] Nakagawa et al.[22] have used this property to estimate the position and identity of the state which causes CIP of I_2 (**B**). Their calculations show that the quenching data cannot be reconciled with dissociation via the $^1\Pi$ (1_u) state. Instead they propose

deactivation via the $^3\Pi$ (0^-_u) state, and provide a potential energy curve which reproduces the observed trend of increasing quenching rate constants with decreasing vibrational energy.

It is probable that the gas phase, solution phase, and matrix quenchings of I_2 (**B**) all proceed by the same mechanism.[23] Contrary to previous assumptions,[24-28] this implies that predissociation via $^1\Pi$ (1_u) is unimportant in condensed media. Recent studies of the analogous predissociation of Br_2 (**B**)[8-11] lend strong support to this idea. Bondybey and Brus[13] have also shown that transfer between the **B** and $^1\Pi(1_u)$ states of ICl does not occur in Ne or Ar matrices.

In the present context it is interesting to note two significant differences between the relaxation dynamics of matrix isolated I_2 and Br_2. First, the lowest levels of Br_2 (**B**) (v'=0, 1) cannot predissociate as they lie below the ground state dissociation limit. Consequently the **B-X** emission spectrum is structured,[8-11] and the v'=0 level decays at the radiative rate.[8] Above the dissociation limit rapid non-radiative decay competes with vibrational relaxation. This behavior is fully in accord with a gas-phase CIP quenching model.[29] Secondly, predissociation of Br_2 (**B**) does not lead to population of the **A** or **A'** states,[9-11] whereas predissociation of I_2 (**B**) does lead to population of I_2 (**A**). This point is of relevance to the previous analyses of the I_2 recombination dynamics in condensed media.[4, 24-28] In essence, the kinetic models used have not been sensitive to the identity of the state causing predissociation, provided that restrictions on the states into which recombination could occur were not imposed. Thus re-assignment of the state responsible for the predissociation of I_2 (**B**) does not require a re-analysis of the recombination kinetics.

(iii) Atomic I^* ($^2P_{1/2}$) → I ($^2P_{3/2}$) Emission

Gas-to-matrix shifts of the atomic I^* ($^2P_{1/2}$) → I ($^2P_{3/2}$) line are given in Table 3. The line was red-shifted by an amount which was directly proportional to the polarizability of the matrix host. This point is illustrated in Table 3, where the matrix shift divided by the polarizability yields an approximately constant value. (The red-shift of the I_2 **A→X** transition does not correlate in such a precise manner, but this is not surprising as the diatomic will be subject to a more complex interaction with the host).

Single photon excitation of the atomic line was noted at wavelengths which did not provide sufficient energy for the channel

$$I_2 (X) + h\upsilon \rightarrow I^* (^2P_{1/2}) + I (^2P_{3/2})$$

Excitation spectra for the atom followed the I_2 **(A)** absorption spectrum, indicating excitation by energy transfer. The near-resonant nature of this transfer is obvious from Fig. 4, where the atomic feature is superimposed on the **A→X**, 0→15 band. Additional support for the transfer mechanism was provided by the observation that atomic emission only appeared in the higher concentration matrices. Prolonged sample excitation did not increase the relative intensity of the atomic line. This is in agreement with the high quantum yield for geminite recombination, and the notion that heavy atoms such as I do not diffuse in rare gas matrices. Thus, free atoms must have been trapped during the deposition process.

The I_2 **(A)**→I^* energy transfer is similar to the Ne matrix Cu_2 **(a)**→Cu^* transfer reported by Bondybey and English.[30] Both are probably mediated by a "Forster type" interaction involving solvation effects and high order multipole coupling. The 5±1 ms lifetime of I^* in Ar and Xe matrices is much shorter than the lifetimes extrapolated from the gas-phase value of ~100 ms[31] (τ_{Ar}~63, τ_{Xe}~47 ms).

No doubt interaction with nearby I_2 molecules, which must be reasonably close in order to effect the initial transfer, is responsible for the accelerated decay.

Energy transfer between I^* and I_2 is thought to play an important role in the chemically pumped oxygen iodine laser (COIL).[32-34] Kinetic studies suggest that $I^* \rightarrow I_2$ transfer is involved in the dissociation of I_2.[32] Excitation of I^* by I_2 (**A**) is a process which has not been reported previously, and may be of importance in COIL. It is known that appreciable concentrations of I_2 (**A**) are present in the laser.[32] Previous models of the lasing kinetics have considered the role of I_2 (**A**) in the dissociation of I_2, but its participation in the direct excitation of I^* has never been examined. The present results indicate that studies of the gas-phase I_2 (**A**) + I system are needed for a more complete understanding of the lasing kinetics.

(iv) Emission Spectra of Iodine Aggregates

Resolved fluorescence spectra for the long-lived emission system seen in concentrated matrices (Fig. 4) are similar in appearance to the **A-X** bands. Superficially the new spectrum seems to be consistent with the $A' \rightarrow X$ transition, but the concentration dependence shows that the carrier is not simply isolated I_2. Furthermore, if the emitting entity is I_2 (**A'**), it must be strongly perturbed by nearby I atoms or I_2 molecules. There are several details which lead to this conclusion. Beeken et al.[4] reported an infra-red emission from Xe/I_2 (1000:1) matrices which they assigned to the **A'-X** system. Although vibrationally unresolved, this emission was found to be strongest in the 2-3 μm range. This was in good agreement with the expected position of the **A'-X** system. The gas-phase electronic term value for the **A'** state is $T_e(A')=10{,}041.2$ cm^{-1}.[29] Assuming similar Franck-Condon factors for the $A \rightarrow X$ and $A' \rightarrow X$ systems, the most intense bands from I_2 (**A'**, $v'=0$) would terminate on the $25 < v'' < 35$ levels, producing

emission in the 2-3 μm range. Beeken et al.[4] obtained a lifetime of 6.3 ms for Xe/I_2 (A'), which fits well with the general trend of decreasing lifetime with increasing mass in the series Cl_2 (A')(τ_{Ar}=76 ms),[12] Br_2(A')(τ_{Ar}=44 ms),[11] and IF(A')(τ_{Ar}~11 ms).[16]

A substantial blue-shift of the A'(v'=0)→X system would be needed for the spectra of Fig. 4 to be consistent with the A'-X assignment. Interactions with the 'pure' host could not produce this kind of perturbation, but the shift could be caused by interactions with nearby I atoms or I_2 molecules. Perturbations of the ground state are evident from the vibrational intervals. When Eq. (1) was fitted to the band centers from Table 2, anharmonicity constants ($\omega_e x_e''$) of 2.6 ± 0.4 (Ar), 2.2 ± 0.4 (Kr), and 1.6 ± 0.4 cm^{-1} (Xe) were obtained. These values are all more than a factor of two greater than the constants determined from the A-X bands (cf. Table 4). The wider spacings of the long-lived bands, compared to the A-X intervals, suggest transitions which terminate on lower vibrational levels of the ground state. This would be consistent with a reduction of the difference between the A' and X state equilibrium internuclear separations.

However, the excited state cannot be unambiguously assigned to perturbed I_2 (A'). It is possible that the emission originates from I_2 dimers or higher aggregates ($(I_2)_n$), but the present results are not easily reconciled with the CW excitation Raman and fluorescence spectra which have been assigned to these species.[1,3] At the concentrations which were used to record the long-lived band system, Howard and Andrews[1] observed Raman spectra of Rg/I_2 matrices that were dominated by features they ascribed to aggregated iodine. At a ratio of 400:1 ($Ar:I_2$) the principal series of Raman lines could be represented by the vibrational constants ω_e'' = 181 cm^{-1}, and $\omega_e'' x_e''$ = 0.03 cm^{-1}. Two weaker series of lines which exhibited approximately 180 cm^{-1} spacings were seen, starting 238 cm^{-1} (series *a*) and 86 cm^{-1} (series *b*) below the excitation line. Although this pattern was

obtained using several different excitation wavelengths, series *a* and *b* were interpreted as fluorescence spectra.[1] In the light of the present work we suggest that these series were actually Raman lines. In our pulsed excitation experiments we have not observed features which correspond to series *a* or *b*, and our fluorescence spectra show intrinsic linewidths which are much broader than those seen by Howard and Andrews.[1] It is more probable that series *a* and *b* are Raman combination bands, consisting of progressions of the 180 cm^{-1} mode built on low frequency aggregate vibrations. The long-lived emission bands (Fig. 4) have vibrational intervals which exceed 190 cm^{-1}, so it is clear that they do not belong to the aggregated entity that produced the Raman lines.

In a later study, Ault and Andrews[3] reported three additional series of sharp lines in the 760-830 nm range, which they assigned to fluorescence from $(I_2)_n$. Two of these series could be seen in dilute matrices, while the third was present only at higher concentrations. Negative anharmonicity constants were a particularly unusual feature of these series. Searches for these spectra were made in the present study, but only the tail of the diffuse **B-X** system was evident in the 760-830 nm range. Again, the sharpness of the spectra seen by Ault and Andrews[3] suggests that they observed either aggregate Raman bands or fluorescence spectra for species other than $(I_2)_n$.

Beyond the fact that the spectra of Fig. 4 belong to some form of aggregated iodine, nothing definitive can be said concerning the emitting species. From the simplest statistical point of view, isolated dimers ($(I_2)_2$) or I_3 molecules are the most probable carriers of the long-lived emission.

(v) Emission from O_2 $a^1\Delta_g$

The low-lying $b^1\Sigma_g^+$ and a $^1\Delta_g$ states of O_2 are very metastable, with gas-phase radiative lifetimes of 12.7s[35] and 1.08 hr,[36] respectively. In solid oxygen and

Rg/O_2 matrices the **b-X** and **a-X** transitions gain oscillator strength when weakly bound dimers $(O_2)_2$ are formed.[37,38] Consequently, most of the matrix data for electronically excited oxygen reflects the spectroscopy of the dimer. In the present study the O_2 **a→X** transition was seen in rare gas matrices, unshifted from its gas-phase position and radiating with a lifetime in excess of 5s. O_2 (**a**) excitation spectra were essentially continuous in the 530-580 nm range, and they did not contain the sharp $(O_2)_2$ vibronic transition at 577.2 nm reported by Goodman and Brus.[37] These observations indicate that the emission originated from isolated O_2(**a**) molecules.

Resonances due to **b←X** or **a←X** absorption bands were not present in the excitation spectra, which was consistent with the very small oscillator strengths of these transitions, and the fact that direct visible excitation of O_2 in Rg matrices has not been reported previously. Thus we conclude that O_2(**a**) was excited by electronic energy transfer in the O_2/I_2/Rg matrices. Transfer from I_2(**A**), which is the most probable donor, is indicated by the similarity between the O_2(**a**) and I_2(**A**) excitation spectra. Energetically, I_2(**A**, $v'=0$)→I_2(**X**, $v''<10$) transitions are capable of exciting O_2(**a**,$v'=0$). Vibrational relaxation of I_2(**X**) would be extremely rapid in the matrix, effectively preventing back transfer.

Lifetimes for O_2(**a**) observed in O_2/I_2/Rg matrices were very sensitive to the I_2 concentration, and shorter than the gas-phase value by factors ranging from 10^3 to 10^5. The lifetime was inversely dependent on the concentration, suggesting that energy transfer to I_2 or I atoms was the main decay channel. Electronic transfer involving vibrationally relaxed I_2(**X**) (O_2(**a**) + I_2(**X**) → O_2(**X**) + I_2(**A** or **A'**)) is not energetically feasible, but O_2(**a**) could decay by electronic to vibrational energy transfer: O_2(**a**) + I_2(**X**,$v''=0$) → O_2(**X**) + I_2(**X**,$v'' \approx 35$). This process has been observed in the gas-phase,[33] where it is thought to be active in the dissociation of I_2 by multiple collisions with O_2(**a**).

In matrices which contained relatively high concentrations of I_2, the decay of $O_2(a)$ was dominated by energy transfer to I atoms. The analogous gas-phase process is known to be efficient,[32] occurring with a rate constant of 7.6×10^{-11} cm^3 $molecule^{-1}$ s^{-1}. In the condensed-phase $O_2(a) \rightarrow I^*$ transfer was manifest as a lengthening of the I^* lifetime (lifetimes in excess of 20 ms were observed in some matrices). This effect implied that the decay kinetics were governed by the transfer rate for the range of conditions investigated.

The apparent splitting of the $I^* \rightarrow I$ line observed in matrices containing high concentrations of O_2 can be explained in terms of a simple site effect. The high frequency component of the "split" feature always occurred at the position characteristic of oxygen-free matrices, and corresponded to emission from I atoms in local sites that did not contain O_2 nearest neighbors. The intensity of the low frequency component was dependent on O_2 concentration, and corresponded to emission from I atoms perturbed by the presence of nearby O_2 molecules. Emission from both components decayed at the same rate, indicating that energy migration between the different sites was facile in these matrices.

IV. 193 nm Excitation of I_2 in an Ar Matrix

IV. a. Results

Excimer laser excitation (193 nm) of dilute (1000:1) Ar/I_2 matrices produced an intense vibronic feature in the near u.v., the I_2 **A-X** bands, and the $I\ ^2P_{1/2} - ^2P_{3/2}$ line. Fig. 6 shows an example of the near u.v. emission spectrum. The band centered at 380 nm was observed in I_2 containing matrices only, but the broad feature, which peaks at 396 nm, was also present when "pure" Ar matrices were excited. Clearly this feature belonged to a trapped impurity. Lifetime measurements for the 380 nm emission indicated a very fast decay, which was convoluted with the 15 ns response time of the photomultiplier/transient

recorder system. From the slight temporal broadening of the laser profile we estimate a lifetime of 5 ns.

I_2 **A-X** emission and the **I*** atomic line were weakly induced by 193 nm radiation. Excitation of the same matrix samples at 532 nm yielded strong **A-X** spectra, but no sign of the atomic feature.

IV. b. Discussion

In the gas-phase, excitation of I_2 in the region of 193 nm is known to populate states that correlate with the $I^+(^3P)+I^-(^1S)$ ion-pair dissociation limits.[39] The u.v. absorption bands have been carefully analyzed by Tellinghuisen,[40] who concluded that the 193 nm output from an ArF laser excites the $D(0_u^+)$ $144<v'<156$ $X\,^1\Sigma_g^+$ $v''=0$, 1, and 2 transitions. Under low pressure conditions the **D** state relaxes through **D→X** and **D→a'**(0_g^+) emission.[39] However, in the presence of moderate pressures of an inert buffer gas (e.g. 400 Torr Ar), population is rapidly transferred from $D(0_u^+)$ to the lowest vibrational levels of the **D'**(2g) state (the lowest energy state of the first ion-pair cluster), and the emission spectrum is dominated by the **D'-A'** bands.[39] These fall in a compact group centered at 340 nm, with a band contour width (FWHM) of about 30Å (290 cm^{-1}).

Previous studies have shown that ion-pair states are more strongly perturbed by the matrix environment than the valence states.[41-43] For example, Ault and Andrews[41] noted that the Xe^+F^-**(B)→**XeF**(X)** transition in an Ar matrix was hugely red-shifted (4000 cm^{-1}) with respect to the gas-phase spectrum. Similarly, a large red-shift of the I_2 ion-pair states, relative to the valence states, is expected in rare gas matrices. Red-shifting of the I_2 **D-X** transition will strongly enhance the $v''=0$ absorption coefficient at 193 nm.[39] As in the gas-phase, excitation of the **D** state should be followed by rapid relaxation to **D'**(2g)$v'=0$, which will then radiate to the **A'** state. Hence, **D'→A'** is the most likely assignment for the 380

nm band of Fig. 6. The lifetime data is consistent with emission from D' (τ_{gas}=6.7 ns[44]). The matrix red-shift corresponding to this assignment (3100 cm^{-1}) is large, but comparable to the ion-pair/valence shifts reported for the rare gas halides.[41,42] The 70Å (480 cm^{-1}) width of the D'-A' spectrum is more than twice that observed in the gas-phase. Given the large difference between the interactions of the ion-pair and valence states with the host lattice, simple Franck-Condon arguments predict that charge transfer transitions will strongly excite the phonon modes. Consequently, it is probable that phonon broadening is responsible for the increased width of the D'-A' transition in the matrix.

The behavior of u.v. excited I_2 and Cl_2 in Ar matrices appears to be quite similar. Fournier and co-workers[45,46] have studied the emission spectra produced by irradiating Ar/Cl_2 matrices with light in the 120-170 nm range. Absorption at these wavelengths primarily excited the $D(0_u^+)$-$X^1\Sigma_g$ charge transfer transition. Rapid electronic and vibrational relaxation then occurred, followed by emission of a band centered at 310 nm. Fournier and co-workers[45,46] initially assigned this band to a $^3\Pi g \rightarrow 1^3\Sigma_u^+$ transition. However, Le Calve' and Chergui[43] have since provided convincing arguments for assigning the 310 nm emission to the D'-A' system, despite the fact that this implies an impressive matrix red-shift of 6500 cm^{-1}.

It is most unlikely that I_2(A) is directly accessed by 193 nm light (the maximum of the A-X absorption occurs at 675 nm). Electronic relaxation and dissociation/recombination sequences are more probable excitation mechanisms. The D'-A' transition terminates on high vibrational levels of the lower state. Near the dissociation limit there is reasonably good Franck-Condon overlap between the A' and A states, permitting transfer excitation of A. Dissociation of I_2 following 193 nm absorption may occur directly, via excitation of a repulsive

state, or by predissociation during the D→D' transfer process. Recombining I $^2P_{3/2}$ atoms would then populate the A, A', and X states.

193 nm excitation of $I^2P_{1/2}$ in dilute matrices must also be a consequence of electronic energy transfer and/or photodissociation. The atomic feature was not observed when the samples were excited at 532 nm, indicating that the I_2/I concentration was too low for $I_2(A) \rightarrow I^*$ to be a significant process. Long-range energy transfer from the ion-pair states may be involved (Concentration dependence studies will be made to investigate this possibility). Alternatively, dissociation from states correlating with the $I\ ^2P_{1/2} + I\ ^2P_{1/2}$ or $_{3/2}$ limits may occur. As geminite recombination is orders of magnitude faster than I^* radiative decay, the atoms would have to escape the matrix cage in order to be observed in emission. Cage escape is feasible in this situation, as the $I\ ^2P_{1/2} + ^2P_{3/2}$ pair will separate with a recoil energy of approximately 31,000 cm^{-1}.

V. Electronic Spectra of Matrix Isolated IBr

V. a. Results

Visible laser excitation of Ar/IBr matrices yielded two far-red emission systems, radiated with significantly different lifetimes. Fig. 7 shows a fluorescence spectrum recorded with the Ge detector (rise time=30 μs), at a boxcar gate delay of 50 μs. The resolution of this spectrum was not instrumentally limited; the broad structureless contour was a characteristic of the emitting state. When corrected for the wavelength dependent sensitivity of the detector, Fig. 7 indicates a peak in the intensity distribution at about 850 nm. An excitation spectrum for the short-lived emitter is shown in Fig. 8.

The longer-lived emission system was observed using a boxcar gate delay of 0.5 ms. This spectrum, which consisted of a single vibronic emission originating from a v'=0 level, is shown in Fig. 9. The band centers from this trace are listed

in Table 5. A slight broadening of the bands was noticeable at the long wavelength end of the spectrum. The atomic I $^2P_{1/2}$-$^2P_{3/2}$ transition was also evident at 1322 nm.

Reliable determinations of the lifetimes for either emission system could not be made, as the fluorescence decay curves were too severely convoluted with the detector response characteristics. Approximate upper limits for the lifetimes, deconvoluted from the response curve, were 20 μs and 0.2 ms for the bands shown in Figs. 7 and 9, respectively.

V. b. Discussion

The absorption spectrum of IBr within the 450-600 nm range is dominated by the **B-X** transition.[47] All levels of the B state are energetically capable of predissociation, and gas-phase lifetime measurements reveal relatively slow predissociation of v'=2 and 3[19] (lifetimes for v'=0 and 1 have not been determined). An avoided crossing between the **B** state and a repulsive 0^+ state results in rapid predissociation of all levels above v'=5.[19] The Franck-Condon factors for the **B-X** transition are such that transitions from v"=0 to v'<5 are weak.[48] Consequently, our matrix spectra primarily reflect excitation of very unstable **B** state levels. Wavelengths below 545 nm excite the **B-X** continuum.

It is most probable that the short lived fluorescence (Fig. 7) is the **B**(v'=0)-**X** system. The wavelength range and intensity distribution of this spectrum is in good agreement with the spectrum predicted from the gas-phase potential energy curves and Franck-Condon factors.[48] The radiative lifetime of IBr(**B**) is not known, but it is expected to fall in the range of 4±2 μs;[48] well below the upper limit estimated for the matrix emission. As in the case of I_2(**B**) (section III.b), the lifetime of IBr(**B**) in rare gas matrices may be appreciably shortened by non-radiative decay channels. Further support for the **B-X** assignment is provided by

the excitation spectrum. In Fig. 8 the matrix spectrum is compared with the gas-phase continuum absorption spectrum.[49] Apart from a matrix red-shift, the two spectra are closely similar, showing that the emission intensity correlates with **B** state excitation. Comparison of the excitation spectra for matrix isolated IBr(**B**) and ICl(**B**) is also of interest. Levels of ICl(**B**) lying below the $B^3\Pi(0^+)$-$B'(0^+)$ curve crossing are stable, and have high fluorescence quantum yields.[13] Above the curve crossing predissociation greatly reduces the quantum yield. When combined with the absorption profile, this effect produces a minimum in the excitation spectrum in the vicinity of the curve crossing. The corresponding curve crossing in IBr would be expected to influence the **B** state excitation at about 590 nm. Fig. 8 varies monotonically in this region, implying that the **B** state fluorescence quantum yield is not significantly altered by the curve crossing. This contrasting behavior is a consequence of the inherent instability of all levels of IBr(**B**).

Matrix isolated IBr(**B**) and I_2(**B**) both give rise to structureless fluorescence spectra. They are the only members of the family of diatomic halogens and interhalogens to exhibit this characteristic. They are also unique in having B states which lie entirely above the ground state dissociation limit. Evidently, the diffuse nature of the **B**→**X** matrix spectrum is associated with predissociation of the v'=0 level.

Structured fluorescence spectra for matrix isolated IBr have not been reported previously. Wight et al.[14] investigated CW laser excitation of IBr/Ar matrices. They observed a progression of IBr(**X**) resonance Raman bands which defined the vibrational constants ($I^{79}Br$) ω''_e=268.4 and $\omega''_e x''_e$=1.16 cm^{-1} for $0 \leq v'' \leq 10$. The vibrational intervals of the structured fluorescence spectrum seen in the present work (Fig. 9) are consistent with theses constants, indicating a transition which terminates on the IBr ground state. Broadening of the bands at longer

wavelengths, which we attribute to divergence of the $I^{79}Br$ and $I^{81}Br$ energy levels with increasing v", supports this assignment.

To fall within the observed spectral region, the long-lived emission must originate from v'=0 of either the A or A' states. Both have similar R_e values, and their most intense transitions from v'=0 will terminate on v"≈15.[48] Thus, the intensity distribution could be used to obtain an approximate vibrational numbering for Fig. 9. This numbering was refined by fitting the band centers to Eq. (1), and comparing the vibrational constants with those of Wight et al.[14] (as the isotopic splittings could not be resolved in our spectra, the fitted constants correspond to the isotopic mean). The numbering given in Table 5 yields the constants $T_e(A)=12285 \pm 20$, $\omega''_e=268\pm2$, and $\omega''_e x''_e=1.04\pm0.07$ cm^{-1}. Acceptable vibrational constants were also obtained when this numbering was raised or lowered by on unit. The range of T_e values encompassed by these fits ($12080 < T_e < 12560$ cm^{-1}) uniquely identified emitting state as $A^3\Pi(1)$ ($T_e(A)_{gas}=12361$ cm^{-1}). As noted in section II, Ar matrix isolation of diatomic halogens and interhalogens is known to cause red-shifts (with respect to the gas-phase) of the 2431 $^3\Pi$ state T_e values.[16,17] When the numbering of Table 5 was increased by one unit, the fit to Eq. (1) gave a blue-shifted value of $T_e(A)$, which is most improbable. Reducing the numbering by one unit gave the constants $T_e(A)=12019\pm20$, $\omega''_e=266\pm2$, and, and $\omega''_e x''_e=1.04\pm0.07$ cm^{-1}. The gas to matrix red-shifts for the two viable assignments were 80 cm^{-1} and 340 cm^{-1}. Both values are slightly anomalous. For the other halogens and interhalogens red-shifts of 180-250 cm^{-1} are typical. The two alternative numberings give $T_e(A)$ values which are symmetrically displaced from these limits, so there is no objective way of choosing between them.

Preliminary studies of the IBr(A) excitation spectrum indicate a curve which is very similar to Fig. 9. Thus it appears that IBr(A) is efficiently excited by

B→A transfer. This is similar to the dynamics observed for I_2, but it contrasts with the results for Br_2(**B**) and the stable levels of ICl(**B**). Again, these trends can be explained in terms of the relative stabilities of the **B** v'=0 levels.

References

1. W. F. Howard and L. Andrews, J. Raman Spectrosc. 2, 447 (1974)
2. J. M. Grzybowski and L. Andrews, J. Raman Spectrosc. 4, 99 (1975)
3. B. S. Ault and L. Andrews, J. Mol. Spectrosc. 70, 68 (1978)
4. P. B. Beeken, E. A. Hanson, and G. W. Flynn, J. Chem. Phys. 78, 5892 (1983)
5. B. S. Ault, W. F. Howard, and L. Andrews, J. Mol. Spectrosc. 55, 217 (1975)
6. M. Mandich, P. Beeken, and G. W. Flynn, J. Chem. Phys. 77, 702 (1982)
7. P. B. Beeken, M. Mandich and G. W. Flynn, J. Chem. Phys. 76, 5995 (1982)
8. V. E. Bondybey, S. S. Bearder, and C. Fletcher, J. Chem. Phys. 64, 5243 (1976)
9. J. P. Nicolai, L. J. van de Burgt, and M. C. Heaven, Chem. Phys. Lett. 115, 486 (1985)
10. J. P. Niclolai and M. C. Heaven, J. Chem. Phys. 83, 6538 (1985)
11. J. Langen, K. -P. Lodeman, and U. Schurath, Chem. Phys. 112, 393 (1987)
12. V. E. Bondybey and C. Fletcher, J. Chem. Phys. 64, 3615 (1976)
13. V. E. Bondybey and L. E. Brus, J. Chem. Phys. 62, 620 (1975); J. Chem. Phys. 64, 3724 (1976)
14. C. A. Wight, B. S. Ault, and L. Andrews, J. Mol. Spectrosc. 56, 239 (1975)
15. J. C. Miller and L. Andrews, J. Mol. Spectrosc. 80, 178 (1980)
16. J. P. Nicolai and M. C. Heaven, J. Chem. Phys. 87, 3304 (1987)
17. M. E. Jacox, J. Mol. Struct. 157, 43 (1987)
18. J. Tellinghuisen, J. Chem. Phys. 76, 4736 (1982)
19. M. C. Heaven, Chem. Soc. Rev. 15, 405 (1986)
20. M. A. A. Clyne and M. C. Heaven, J. Chem. Soc. Faraday Trans. 2, 76, 117 (1980)
21. *J. I. Steinfeld, Acc. Chem. Res. 3, 313 (1970)*

22. K. Nakagawa, M. Kitamura, K. Suzuki, and T. Kondow, Chem. Phys. 106, 259 (1986)

23. J. Tellinghuisen, J. Chem. Phys. 82, 4012 (1985)

24. D. F. Kelley, N. Alan, Abdul-Haj, and Du-Jeon Jang, J. Chem. Phys. 80, 4105 (1984)

25. J. -C. Dutoit, J. M. Zellweger, and H. van den Bergh, J. Chem. Phys. 78, 1825 (1983)

26. M. W. Balk, C. L. Brooks and S. A. Adelman, J. Chem. Phys. 79, 804, (1983)

27. D. P. Ali and W. H. Miller, Chem. Phys. Lett. 105, 501 (1984)

28. J. M. Dawes and M. G. Sceats, Chem. Phys. 96, 315 (1985)

29. M. Kitamura, K. Nakagawa, K. Suzuki, T. Kondow, K. Kuchitsu, T. Munakata, and T. Kasuya, J. Phys. Chem. 90, 1589 (1986)

30. V. E. Bondybey and J. H. English, J. Phys. Chem. 87, 4647 (1983)

31. F. J. Comes and S. Pionteck, Chem. Phys. Lett. 42, 558 (1976)

32. R. F. Hiedner, C. E. Gardner, C. E. Gardner, G. I. Segal, and T. M. El-Sayed, J. Phys. Chem. 87, 2348 (1983)

33. M. H. van Bentham and S. J. Davis, J. Phys. Chem. 90, 902 (1986)

34. G. E. Hall, W. J. Marinelli, and P. L. Houston, J. Phys. Chem. 87, 2153 (1983)

35. P. H. Krupenie, J. Phys. Chem. Ref. Data, 1, 426 (1972)

36. R. M. Badger, A. C. Wright, and R. F. Whitlock, J. Chem. Phys. 43, 4345 (1965)

37. J. Goodman and L. E. Brus, J. Chem. Phys. 67, 4398 (1977)

38. H. Frei and G. C. Pimentel, J. Chem. Phys. 79, 3307 (1983)

39. J. Tellinghuisen and L. F. Phillips, J. Phys. Chem. 90, 5108 (1986)

40. J. Tellinghuisen, Can. J. Phys. 62, 1933 (1984)

41. B. S. Ault and L. Andrews, J. Chem. Phys. 65, 4192 (1976)

42. J. Goodman and L. E. Brus, J. Chem. Phys. 65, 3808 (1976)

43. J. Le Calve and M. Chergui, Chem. Phys. Lett. 132, 256 (1986)

44. M. C. Sauer, W. A. Mulac, R. Cooper, and F. Grieser, J. Chem. Phys. 64, 4587 (1976)

45. J. Fournier, F. Salama, and R. J. Le Roy, J. Phys. Chem. 89, 3530 (1985)

46. F. Salama and J. Fournier, Chem. Phys. Lett. 120, 35 (1985)

47. J. A. Coxon in 'Molecular Spectroscopy', ed. R. F. Barrow, D. A. Long and D. J. Millen, Specialist Periodical Reports, The Chemical Society, London 1973 Vol. 1, p. 177

48. M. A. A. Clyne and M. C. Heaven, J. Chem. Soc., Faraday Trans. 2, 76, 49 (1980)

49. D. J. Seery and D. Britton, J. Phys. Chem. 68, 2263 (1964)

Table 1

Vibronic band positions (cm^{-1}) of the A-X system of I_2 in rare gas matrices.

v'=0→ v''	υ(Ar)	υ(Kr)	υ(Xe)
10	8532	8308	
11	8331	8124	7955
12	8142	7924	7770
13	7947	7734	7588
14	7754	7553	7396
15	7565	7364	7202
16	7372	7179	7024
17	7180	6985	6841
18	6995	6798	6652
19	6807	6623	6472
20	6622	6443	6293
21	6441	6263	6118
22	6256	6086	5942
23	6075	5920	
24	5895		

Table 2

Vibronic band positions (cm^{-1}) for the long-lived emission from 300:1, Rg:I_2 matrices.

υ(Ar)	υ(Kr)	υ(Xe)
7530	7320	7189
7320	7115	6993
7122	6914	6798
6925	6720	6610
6734	6530	6423
6550	6340	6238
6369	6157	6060
6192	5980	5882

Table 3

Line Centers and Matrix Shifts for the $I^*(^2P_{1/2}) \rightarrow I(^2P_{3/2})$ Transition in Rare Gas Matrices.

Host	Polarizability[a] (α; Å^3)	Line Center (cm^{-1})	Matrix shift[b] ($\Delta\upsilon$; cm^{-1})	$\Delta\upsilon$/å
Ar	1.64	7564	41	25
Kr	2.48	7541	64	26
Xe	4.04	7502	103	25

a. T. M. Miller and B. Bederson, Adv. At. Mol. Phys. 13, 1 (1977)

b. The $I^* \rightarrow I$ transition occurs at 7605 cm^{-1} in the gas-phase

Table 4

Spectroscopic constants (cm^{-1}) for the **A-X** system of I_2 in rare gas matrices.

Host	ω_e''	$\omega_e x_e''$	$T_e(A)^a$	Δ^b
Ar	213 ± 4	0.7 ± 0.1	10,660	247
Kr	212 ± 4	0.8 ± 0.1	10,610	297
Xe	207 ± 5	0.7 ± 0.1	10,400	507
gas-phase	214.5	0.61	10,906.8	-

a. Determined using the gas-phase value of $G'(0) = 46cm^{-1}$. Standard deviation ± 40 cm^{-1}.

b. Δ = difference between the gas-phase and matrix values for $T_e(A)$.

Table 5

Vibronic band positions of the **A-X** system of IBr in an Ar matrix.

v'=0→ v"[a]	υ(cm^{-1})[b]
8	10,152
9	9,901
10	9,662
11	9,416
12	9,174
13	8,929
14	8,688
15	8,453
16	8,224
17	7,980
18	7,770
19	7,530
20	7,315
21	7,072
22	6,849
23	6,640
24	6,435
25	6,203

a. The vibrational numberings may be one unit lower than the indicated values. See text for details.

b. Isotopic mean.

Figure Captions

Figure 1. Resolved fluorescence spectra for the I_2 **A - X** system. Rg :I_2 = 2000:1, 532 nm excitation, 0.5 ms boxcar gate delay.

Figure 2. The smooth curve is an excitation spectrum for I_2 (**A**) in an Ar matrix (Ar:I_2 = 1000:1), recorded by monitoring the 1430 nm emission feature. The solid squares represent the absorption spectrum for matrix isolated I_2 reported by Grzybowski and Andrews.[2] The solid circles represent the room temperature absorption spectrum of gas phase I_2, from the work of Tellinghuisen.[29]

Figure 3. Resolved fluorescence spectra from 300:1, Rg:I_2 matrices. 532 nm excitation, 20 ms boxcar gate delay.

Figure 4. Resolved fluorescence spectrum from a 600:1, Ar:I_2 matrix. 532 nm excitation, 2 ms boxcar gate delay.

Figure 5. Resolved fluorescence spectrum from a Xe/O_2/I_2 matrix. 532 nm excitation, 20 ms boxcar gate delay.

Figure 6 Resolved fluorescence spectrum from a 1000:1, Ar:I_2 matrix. 193 nm excitation, boxcar gate synchronous with the laser pulse.

Figure 7 Resolved fluorescence spectrum from an Ar/IBr matrix. 532 nm excitation, 50 μs boxcar gate delay.

Figure 8 The squares represent an excitation spectrum from an Ar/IBr matrix. They were obtained by monitoring the emission intensity at 970 nm, with a boxcar gate delay of 50 μs. The smooth curve is the gas-phase continuum absorption spectrum taken from reference 49.

Figure 9 Resolved fluorescence spectrum from an Ar/IBr matrix. 420 nm excitation, 0.5 ms boxcar gate delay.

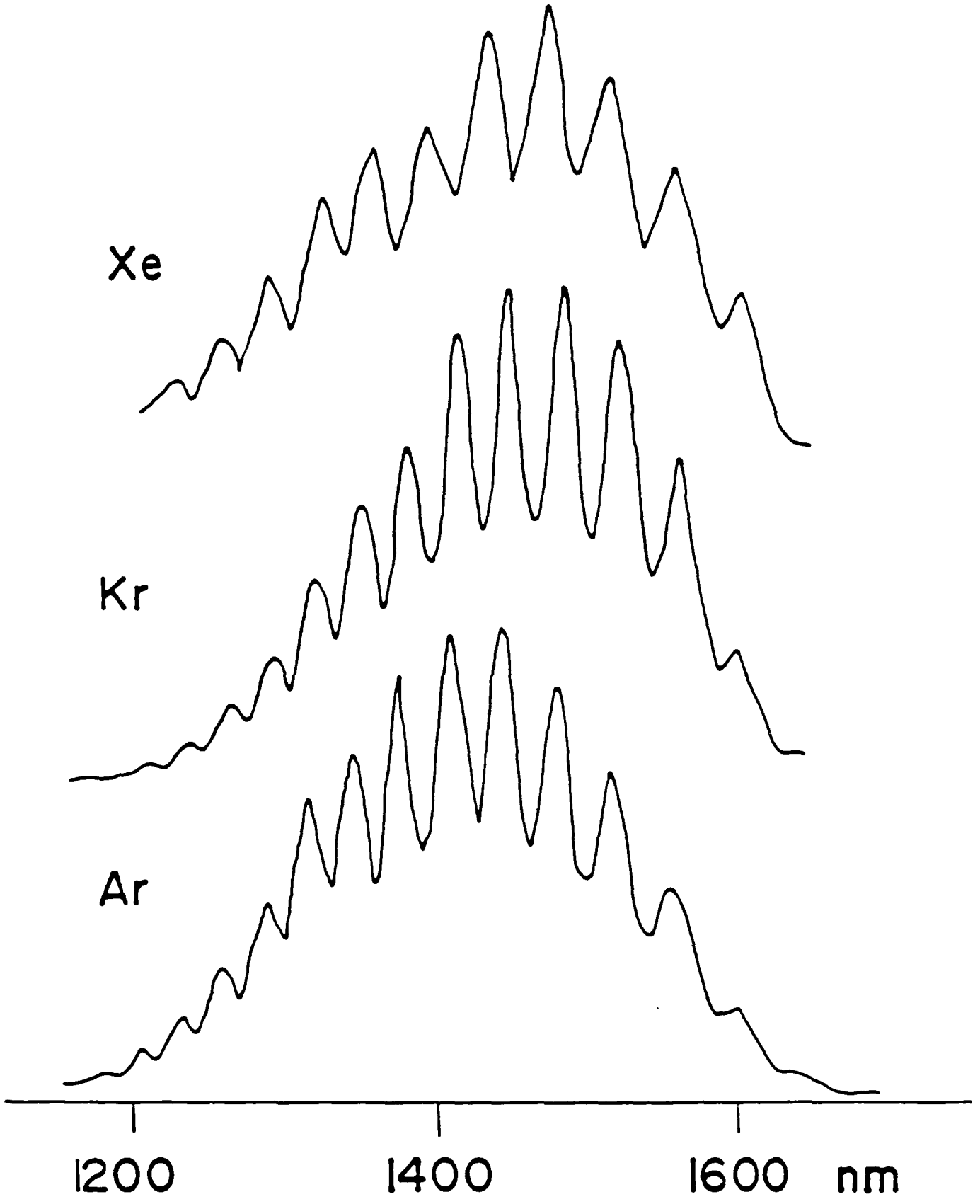
Xe
Kr
Ar
1200
1400
1600
nm

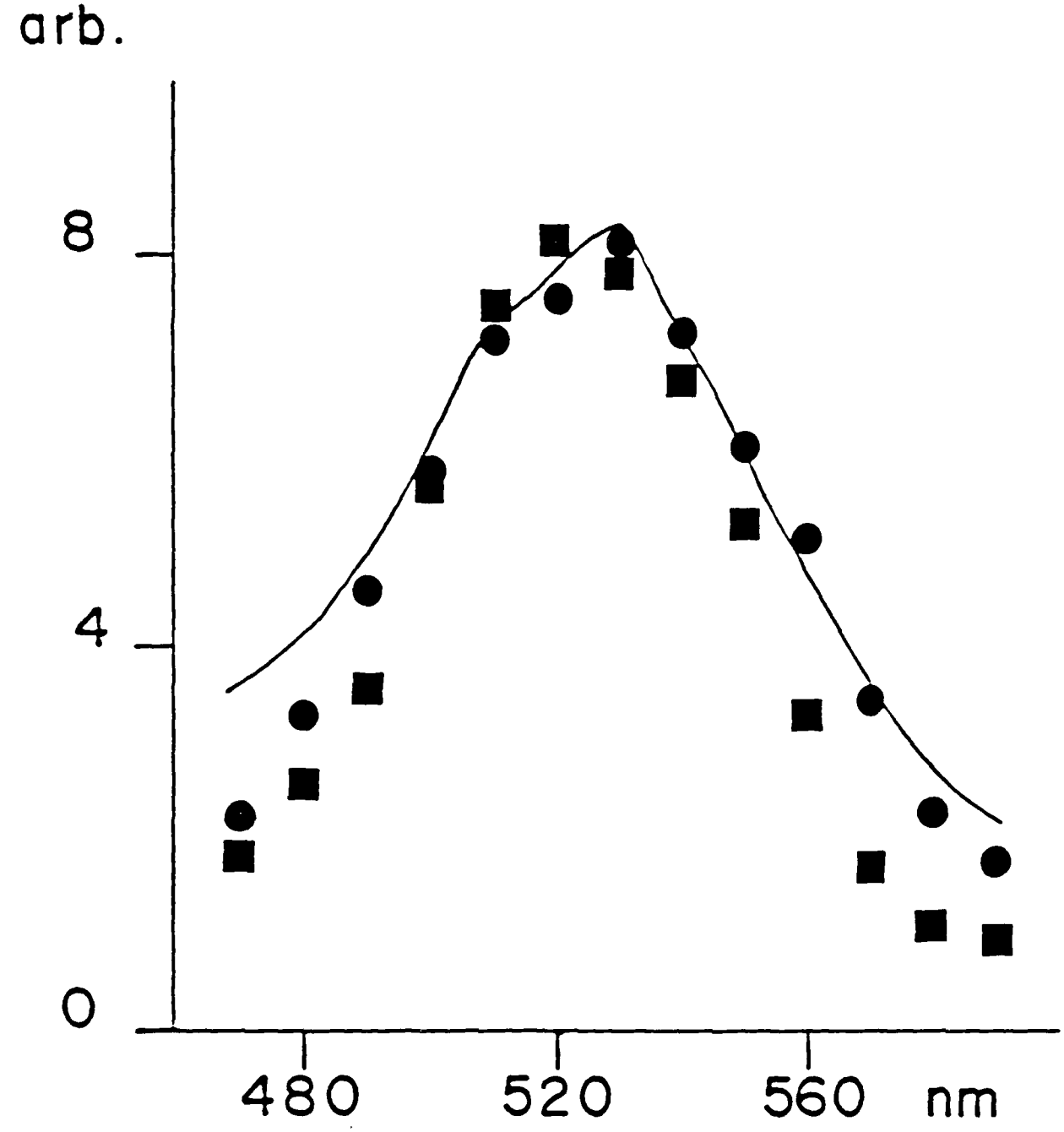
arb.
8
4
0
480
520
560
nm

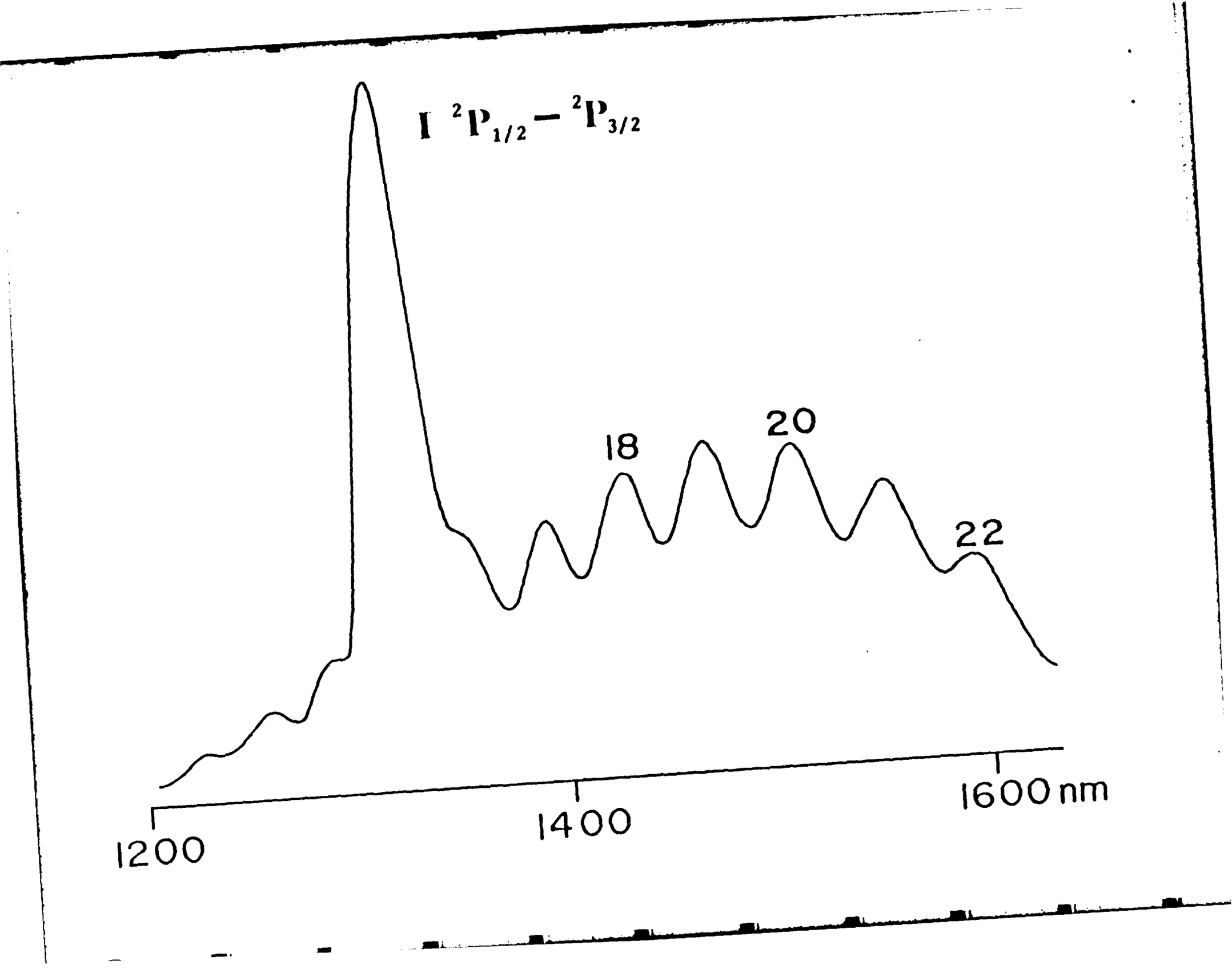
I $^2P_{1/2} - {}^2P_{3/2}$
18
20
22
1200
1400
1600 nm

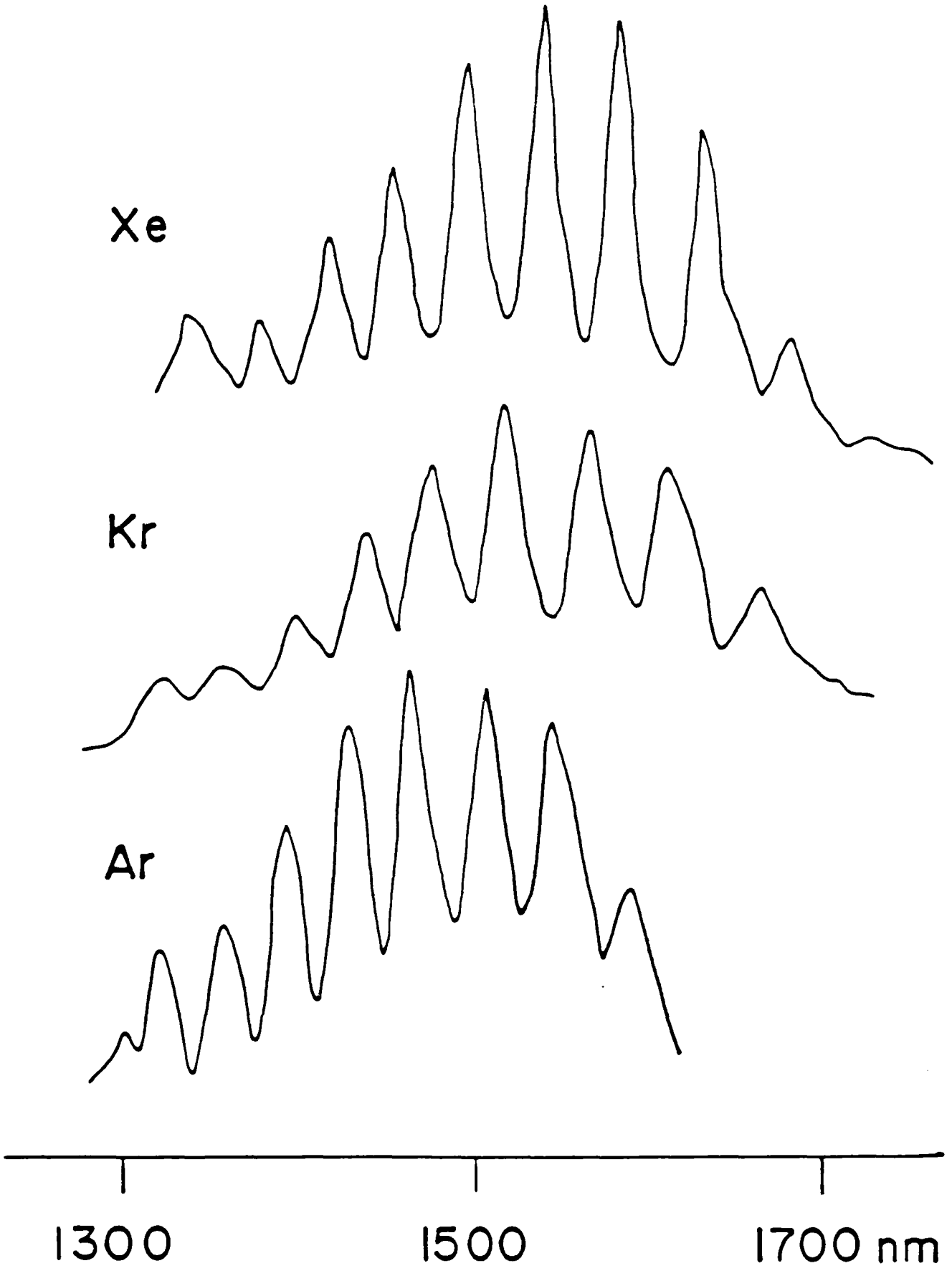
Xe
Kr
Ar
1300
1500
1700 nm

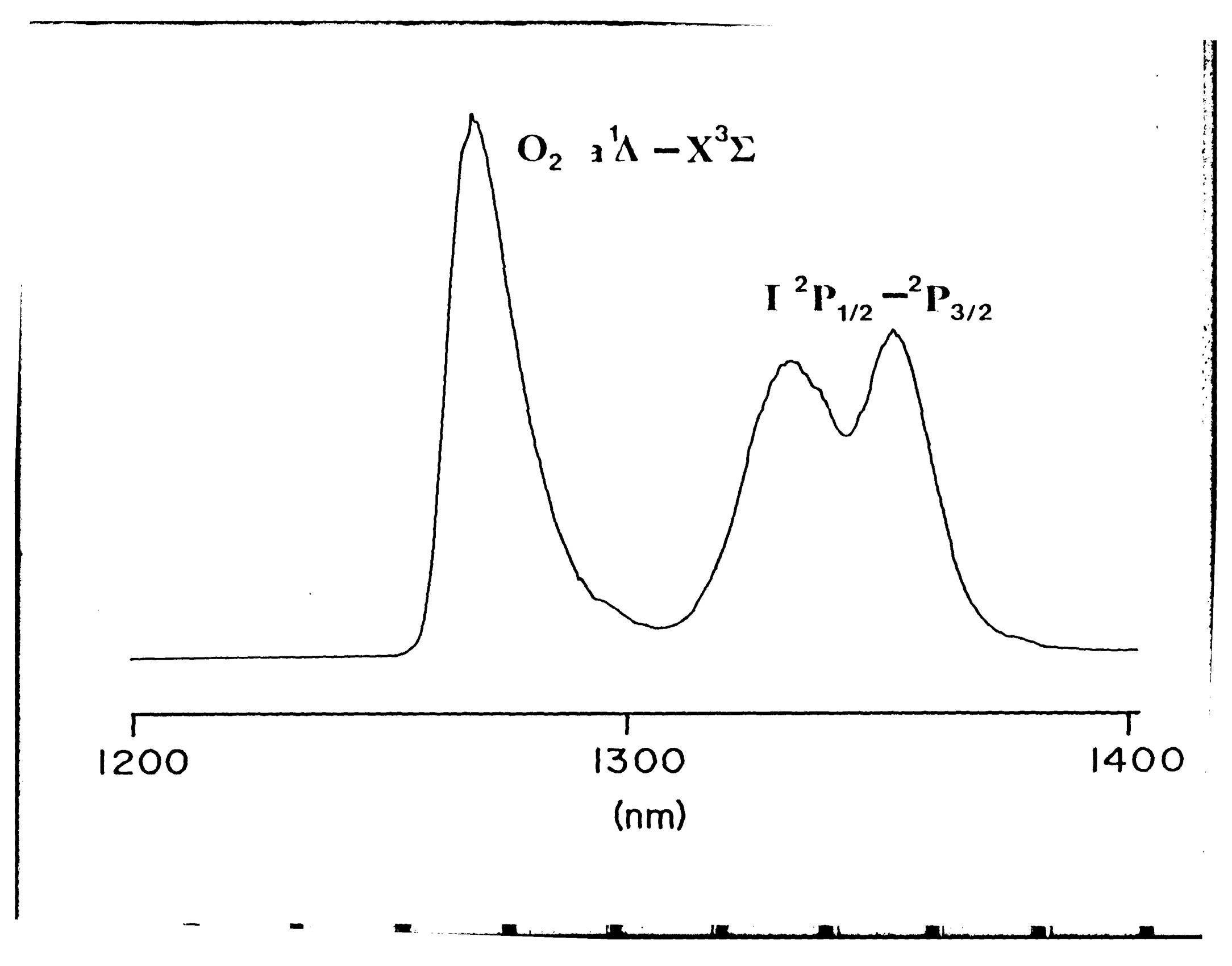
O_2 $a^1\Delta - X^3\Sigma$
$I\ ^2P_{1/2} - ^2P_{3/2}$
1200
1300
1400
(nm)

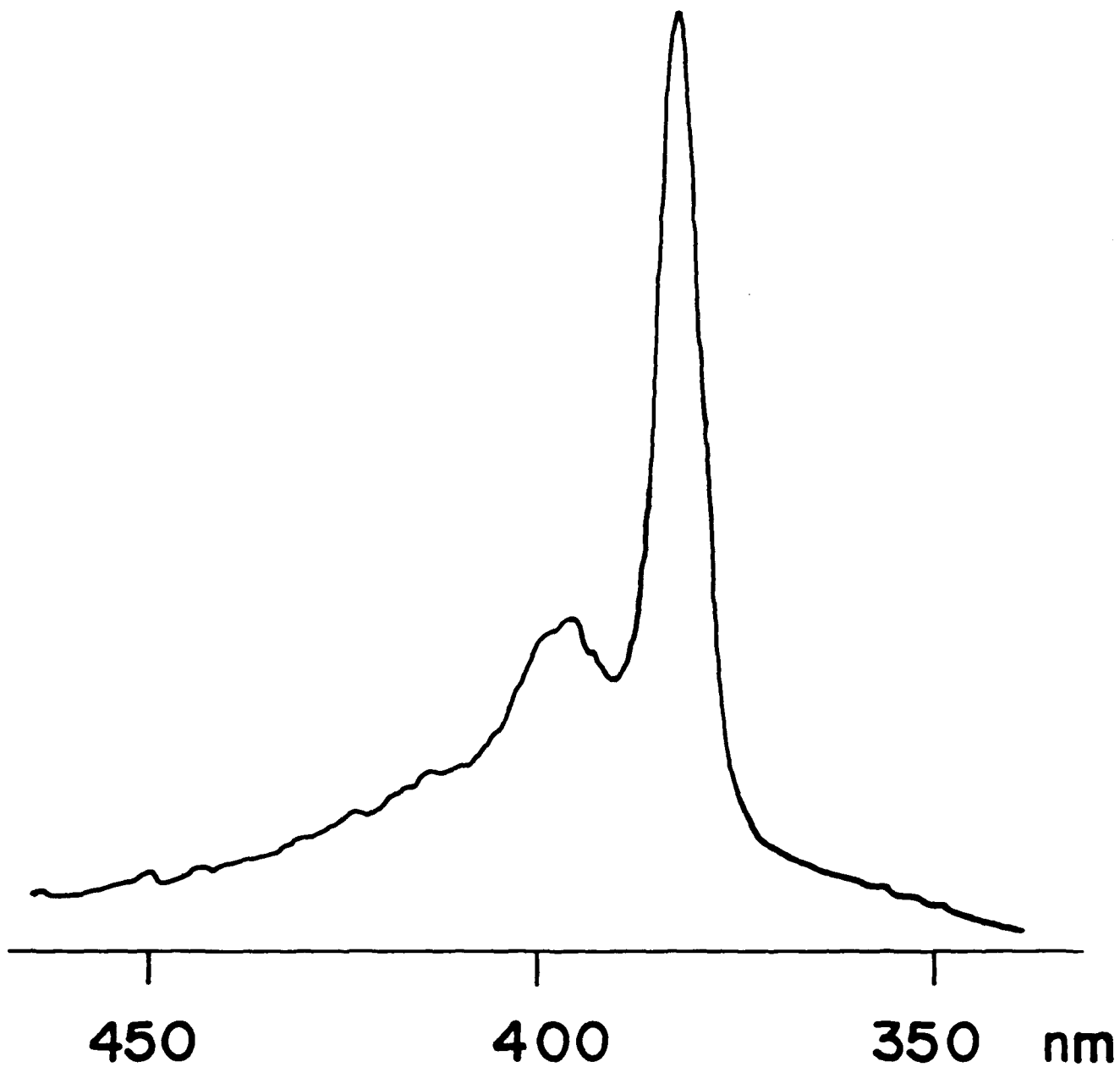
450
400
350
nm

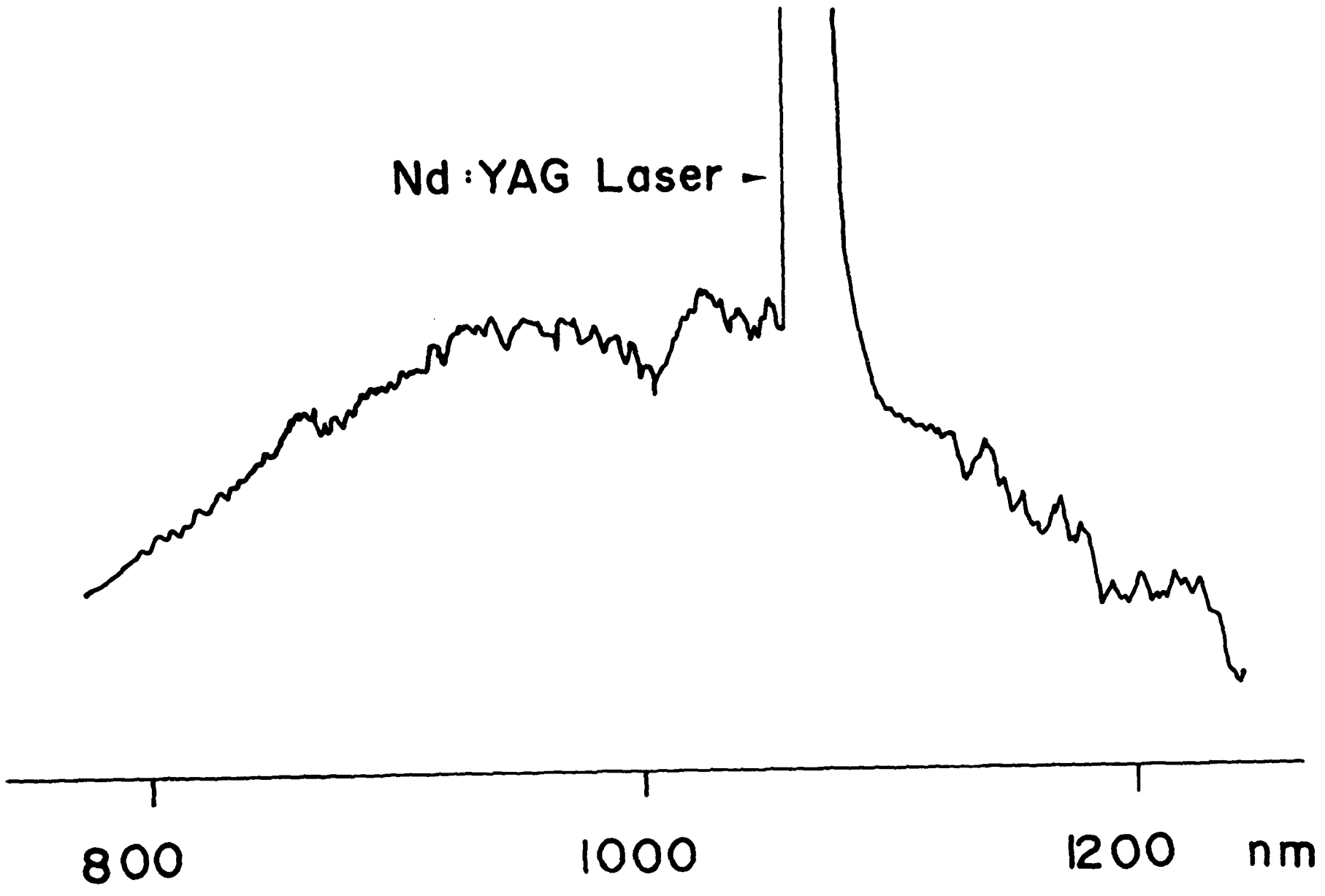
Nd:YAG Laser
800
1000
1200
nm

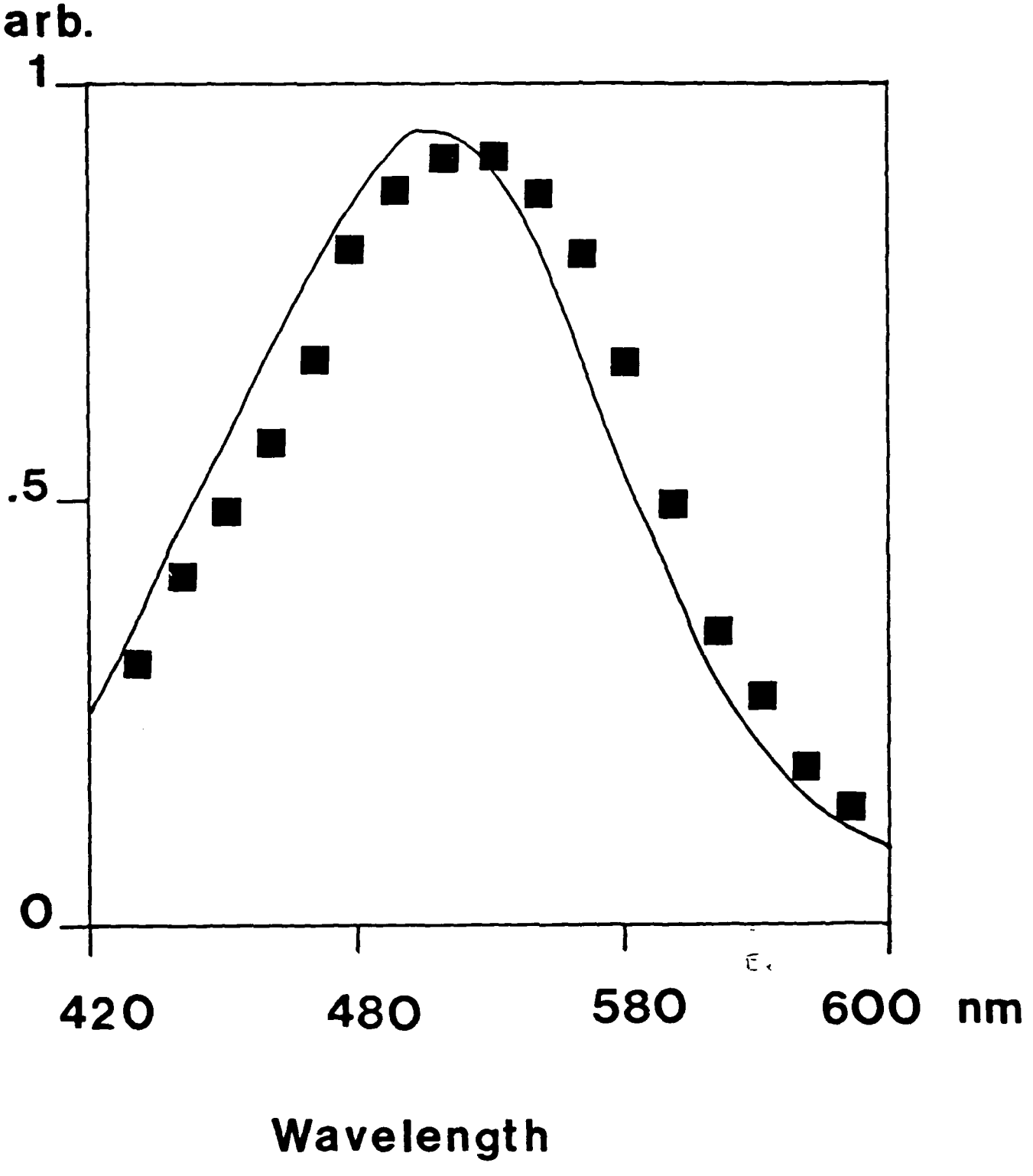
arb.
1
.5
0
420
480
580
600
nm
Wavelength

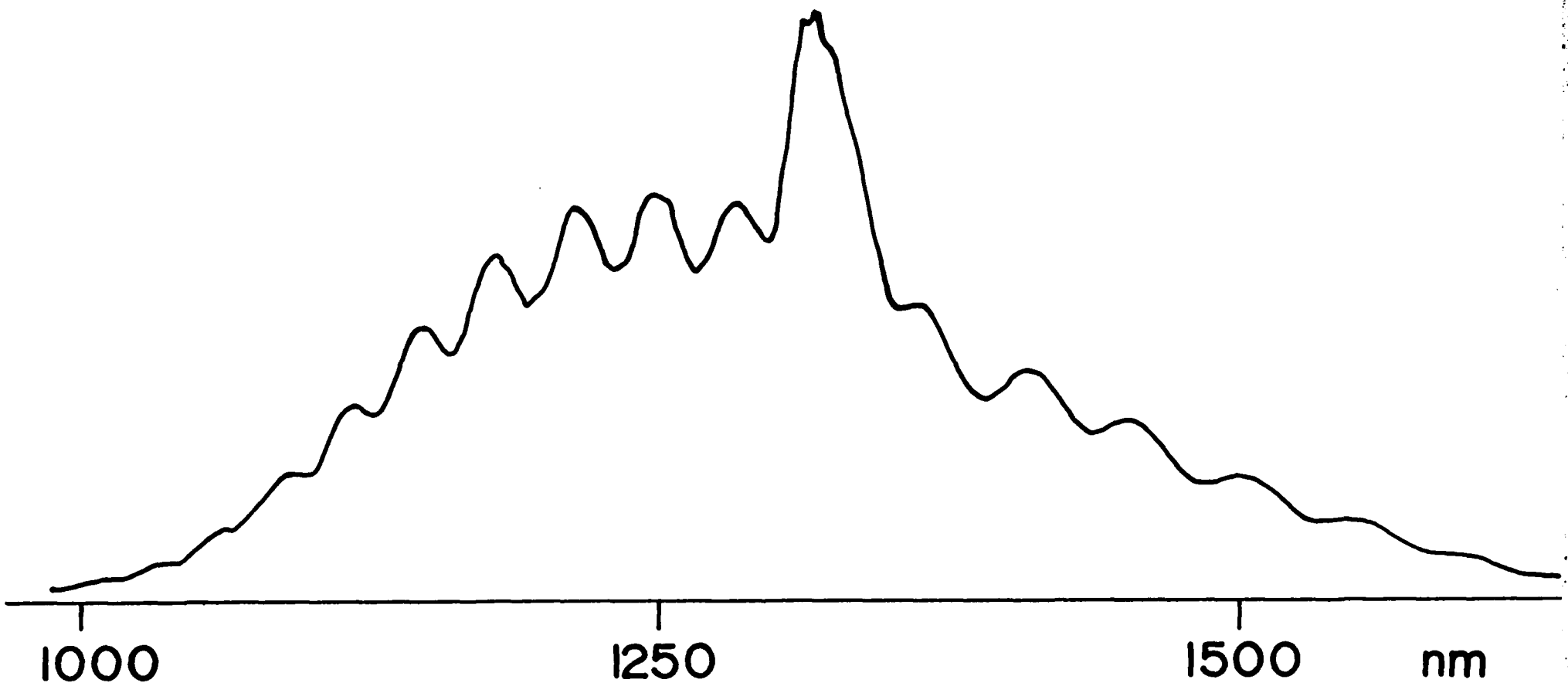
1000
1250
1500
nm